THERMAL CYCLING FIBER METAL LAMINATES: CONSIDERATIONS, TEST SETUP AND RESULTS

B. Müller[1], S. Teixeira De Freitas[2] and J. Sinke[3]

[1]Structural Integrity & Composites, Delft University of Technology,
Kluyverweg 1, 2629 HS Delft, The Netherlands
Email: b.muller@tudelft.nl, web page: http://www.lr.tudelft.nl

[2] Structural Integrity & Composites, Delft University of Technology,
Kluyverweg 1, 2629 HS Delft, The Netherlands
Email: S.TeixeiraDeFreitas@tudelft.nl, web page: http://www.lr.tudelft.nl

[3] Structural Integrity & Composites, Delft University of Technology,
Kluyverweg 1, 2629 HS Delft, The Netherlands
Email: J.Sinke@tudelft.nl, web page: http://www.lr.tudelft.nl

Keywords: Fiber metal laminates; GLARE; thermal cycling; thermal fatigue; moderate temperatures; heater elements; test setup

ABSTRACT

The development of fiber metal laminates to multi-functional materials by embedding heater elements in the laminate extends their field of application. Fiber metal laminates with embedded heater elements are likely to be used for the de- and anti-icing of leading edges in aircraft as they combine structural and heating functions. Hence, those heated fiber metal laminates are exposed to frequent temperature changes when the de- or anti-icing devices are switched on. In order to examine the possible effects of thermal fatigue loading on the material characteristics, a thermal cycling setup was developed. The experimental setup has the ability to perform thermal cycling tests of materials with and without embedded heater elements. For structural materials, the thermal cycling setup provides external cooling and external heating using Peltier elements. For multi-functional materials (materials with embedded heater elements), the experimental setup enables thermal cycling tests by providing external cooling using Peltier elements and internal heating using the embedded heater mesh. The multi-functional material which is thermal cycled in this study is heated GLARE (Glass Laminate Aluminum Reinforced Epoxy). The temperatures recorded by thermo couples at different specimen positions are presented. The thermal cycle times were about 62 s for temperature cycles from 0°C to 60°C and 2 mm thick heated GLARE specimens. Similar thermal cycling times can be reached for both external cooling and heating and external cooling and internal heating. However, the use of Peltier elements to heat the specimens outer surfaces (external heating) leads to more homogeneous temperature distributions than when using the embedded heater elements as internal heating. The presented experimental setup can be adapted to different specimen dimensions, enables thermal cycling of multiple specimens of the same material, and is applicable for different temperature ranges and heating or cooling rates.

1 INTRODUCTION

Testing thermal fatigue, i.e. exposing materials and structures to frequent temperature changes, has been a research topic for decades [5,8]. The research focused on the effects of thermal cycling on the material characteristics and on the structural integrity of components [15]. Thermal cycling tests with different heating and cooling methods, for different heating and cooling rates and different dwelling times were developed [9,19].

Besides from structural materials which are used e.g. in aircraft [5,7], thermal fatigue is also an issue in materials for dental care [9] and electronic parts [19]. The alternating thermal loading of

materials used for dental care and the combination (by bonding) of different materials combined with safety issues result in high demands on the material [25] and adhesive properties [12]. In the case of electronic parts, the investigation of thermal fatigue on the local (material) and the global (component) level is relevant [21]. The change of material characteristics is likely to change both the structural integrity and performance of (electronic) parts.

Advances in the development of multi-functional materials which are likely to be used for the de- and anti-icing of leading edges in aircraft combine structural and heating functions [3,7,16]. Either heater elements are embedded in the prepreg layers of fiber metal laminates (FMLs) or electrically conductive fibers are heated using electrical power in fiber reinforced polymers. This study focuses on the first solution. Figure 1 shows the multi-functional fiber metal laminate heated GLARE which is investigated in this study. GLARE is the acronym of GLAss fiber REinforced Aluminium laminate and is composed of alternating layers of Aluminium and S-2 fiber glass prepregs [23,27,28,29]. Heated GLARE is a fiber metal laminate material in which a copper mesh is embedded between the unidirectional (UD) prepreg layers [7]. To enhance the de- and anti-icing capabilities (heating) of leading edges, the copper mesh is positioned in the UD layers between the outer two Aluminium layers in the heated GLARE laminate. Moreover, numerous studies were conducted which studied the material characteristics of GLARE including fatigue and damage tolerance issues [2], thermal material properties [10] and the thermal diffusion [17].

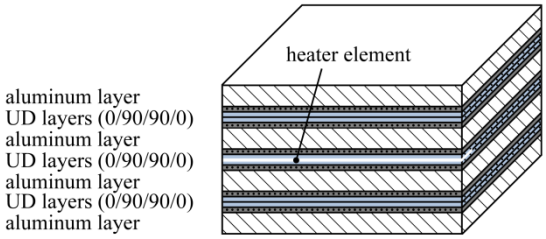

Figure 1: Heated GLARE 5-4/3-0.3 laminate

The development of multi-functional materials used for the de- and anti-icing of leading edges in aircraft [7] encourages the development and design of experimental setups which are reliable and capable to simulate flight conditions. The thermal loading conditions of heated FMLs due to flight conditions can be divided into thermal cycling due to the ascent and descent of aircraft (external cooling and heating) and thermal cycling due to (local) heating of the leading edges by de- and anti-icing measures (external cooling and internal heating). Thus, an experimental setup to investigate both thermal loading conditions is required.

The novelty of the thermal cycling setup introduced in this article is the ability to perform thermal cycling of materials with and without embedded heater elements. For structural materials the thermal cycling setup provides external cooling and external heating. For multi-functional materials (materials with embedded heater elements), the experimental setup enables thermal cycling tests by providing external cooling and internal heating. The multi-functional material which is thermal cycled in this study is heated GLARE (see Figure 1). In order to simulate flight conditions for multi-functional materials, the experimental setup can be adopted to provide constant external cooling using the Peltier elements and frequent internal heating using the embedded heater elements.

2 DEFINITION OF THERMAL FATIGUE TESTS FOR HEATED GLARE

2.1 Requirements and considerations

This study focuses on the design of thermal fatigue tests to simulate flight conditions of leading edges made of heated GLARE. Heated GLARE is likely to be used in the leading edges of aircraft for structural and de-/ anti-icing functions. Thus, the test setup needs to be designed to cover the thermal loading during the ascents and descents of aircrafts and due to the (local) heating of the leading edges using the embedded heater mesh. However, the simulation of the (local) thermal loading of heated leading edges made of heated GLARE are the main focus of this study.

Furthermore, the specimen dimensions should be large enough to allow for extensive destructive and non-destructive tests of the material characteristics of all components of heated GLARE and the structural integrity of the whole laminate before and after thermal cycling.

2.2 Thermal loading conditions

The thermal loading of heated GLARE can be divided in three major loading conditions. Figure 2 summarises the thermal loading conditions of heated GLARE. The first major thermal loading of heated GLARE happens during the manufacturing process in the autoclave at temperatures of 180°C and at a pressure of 6 bar. This first thermal loading, from the curing temperature down to room temperature, leads to thermal residual stresses [1,11]. Hence, heated GLARE has a thermal loading history before getting into service in aircraft structures. The second major thermal load is the thermal cycling due to flight conditions of the whole aircraft, i.e. once per flight within a temperature range of -55°C to 80°C [10]. The third major loading of heated GLARE is the thermal cycling due to de- and anti-icing of the heated leading edges by means of the embedded heater elements, i.e. up to several times per flight for temperature ranges of presumably -20°C to 80°C [6,16].

Figure 2 highlights the combination of mechanical (residual stresses and stresses due to flight conditions) and thermal loading during flight conditions. Furthermore, Figure 2 incorporates the temperature range of icing conditions and temperatures limits which might affect the material properties of heated GLARE. The mapped temperatures are the curing and service temperatures of the prepreg material, the temperature range where aging might affect the Aluminium and the temperatures where the properties of the Aluminium layers change considerably due to the moderately high temperatures [24,26].

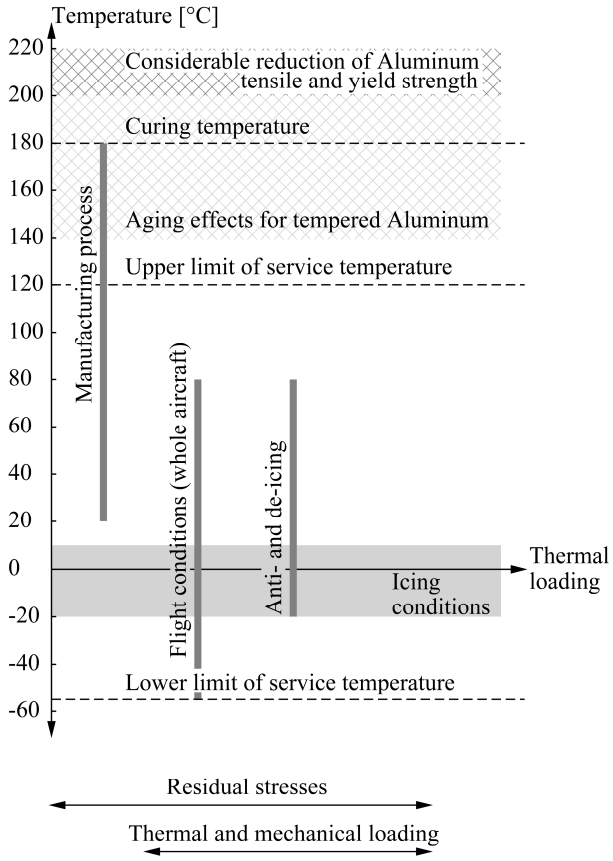

Figure 2: Thermal loading conditions.

2.3 Specimen design

The design parameters for the specimen dimensions and layup are given by the material (heated GLARE), the manufacturing process, the test setup, the kind of coupon tests for examining the possible changes of the material characteristics and the practical application (leading edges). The specimen dimensions in this study are 100 x 100 mm. Figure 3 depicts the specimen dimensions and the position of the embedded copper mesh used for the internal heating. The positions of the embedded thermo couples for the temperature measurements are also indicated.

The specimens' layup used in this study is heated GLARE 5-4/3-0.3, i.e. four layers of Aluminium with 0.3 mm thickness which are bonded together by glass prepreg layers [0/90/90/0], in which the heater elements are embedded in the central composite layer (cf. Figure 1). This leads to a total laminate thickness of approximately 2 mm.

The heater elements are positioned in the center plane of the laminate (see Figure 1). This position is advantageous due to two major reasons. Firstly, this position of the copper mesh in the center plane leads to symmetrical specimen layup. Thus, the internal thermal loading is symmetric in respect to the thickness direction and warping of the specimens due to unsymmetrical thermal loading conditions is reduced to a minimum. Secondly, since interlaminar shear strength tests (ILSS) will be used in a further study to quantitatively assess the material degradation [4] where the maximum shear stresses are expected to occur in the center plane [14]. Thus, the possible effects of both the heater element and thermal fatigue in the vicinity of the heater elements are examined. Furthermore, the laminate thickness of 2 mm fulfils the thickness requirements of ILSS tests.

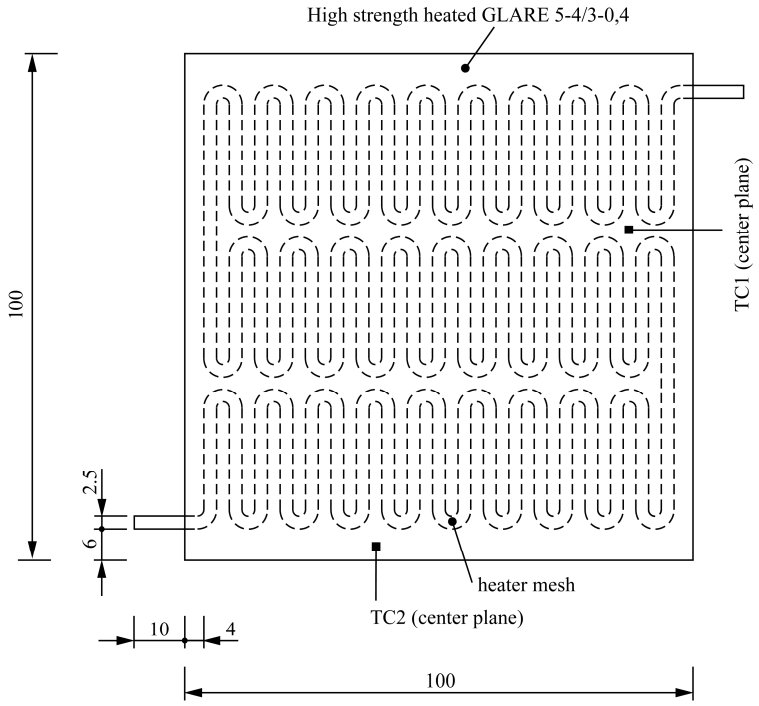

Figure 3: Heated GLARE 5-4/3-0.3 specimen dimensions including the positions of two embedded thermo couples in the center plane (plane where the heater mesh is embedded, cf. Figure 1)

2.4 Experimental setup

The experimental setup is designed to perform thermal fatigue tests for structural materials and multi-functional materials, i.e. for materials which combine structural and heating functions. When testing purely structural materials, e.g. GLARE, the experimental setup provides both external cooling and external heating using Peltier elements. The Peltier elements cool and heat the external surfaces of the specimen. For thermal cycling multi-functional materials (e.g. heated GLARE), the experimental setup provides external cooling and internal heating using the embedded heater elements.

Figure 4 depicts the experimental setup used in this study. The experimental setup consists of one computer, two power supplies, one relay, (embedded) thermo couples, Peltier elements, heat conductive pillows and four heat sinks with attached ventilators. Peltier elements have two sides which when provided with electrical power, one side is cooled (cold side) and the opposite side is heated (hot side) [30]. The cold and the hot side switch positions if the direction of the electrical current (DC) changes. The computer is used to control the power supplies and the relays through the software LabView [13]. The two power supplies and the relay are used to provide the Peltier elements and the embedded heater element with electrical power. The heat sinks and ventilators are used to dissipate the heat produced at the hot side of the Peltier elements when cooling the specimen. Thermo couples are embedded in the specimens and applied on the surface of the specimens and heat sinks to monitor and control the temperature during the thermal cycling tests.

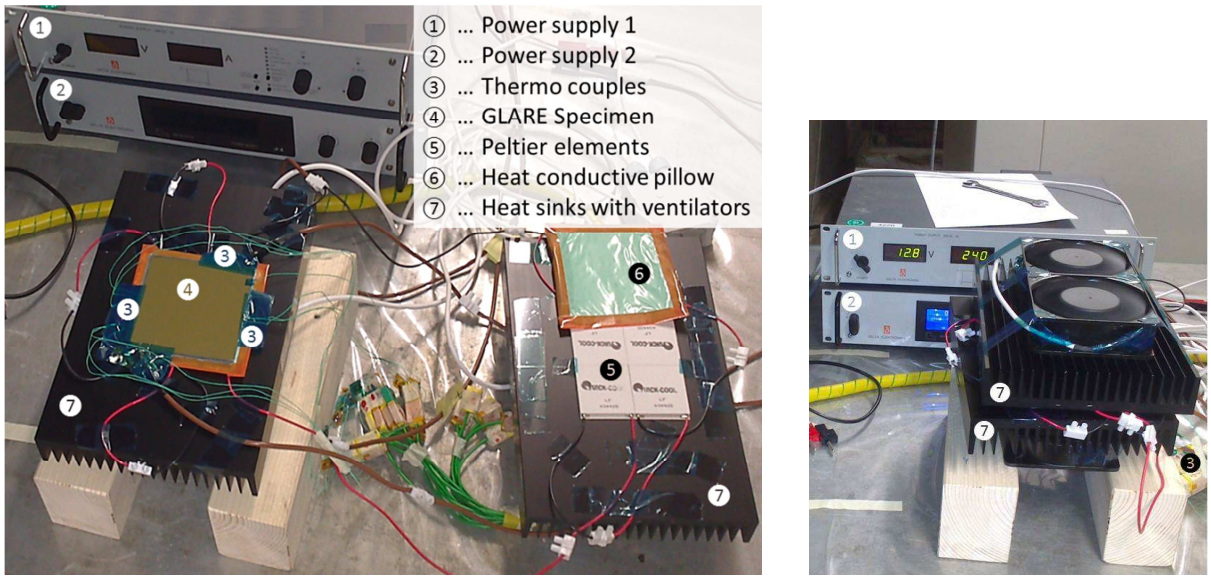

(a) (b)

Figure 4: Experimental setup (a) disabled and (b) during testing.

The main reasons to use Peltier elements are that they can provide both cooling and heating and provide the opportunity to control the heating and cooling power separately, i.e. the temperature increase rates. Furthermore, the use of Peltier elements enables to adopt the setup to different specimen dimensions and temperature ranges by changing the number of Peltier elements. If larger temperature ranges or faster temperature change rates are required, the Peltier elements can be stacked, i.e. mounted in two or more layers. Furthermore, no additional liquids (e.g. cooling liquids with direct specimen contact) are needed which might affect the moisture content of specimens.

The heat conductive pillows were applied on both sides of the specimen to improve the heat conduction between the Peltier elements and the specimen. The heat conductive pillows consist of a thin layer of heat conductive paste wrapped in a thin heat resistant foil. The heat conductive pillows are used to close possible air gaps between the Peltier elements and the specimens. The disadvantage of using these pillows is that the heat conduction might be slightly lower when compared to the direct application of the heat conducting paste on the specimen. However, the clean test environment which is guaranteed by the heat conductive pillows and the exclusion of possible reactions of the specimen surfaces with the heat conducting paste weight against the slightly less heat conduction.

In the case of external cooling and heating, the Peltier elements are used for both heating and cooling (cf. Figure 4). Hence, only one power supply is needed. In order to enable external heating and cooling, the direction of the current is changed using the relay which is controlled by the computer, i.e. the measured temperatures of the thermo couples.

In the case of the external cooling and internal heating, the Peltier elements are used for cooling and the embedded (internal) mesh is used for heating (cf. Figures 3). The cooling and heating are

performed with two different power supplies; both are controlled by the computer using the temperatures measured by the thermo couples. In the case of internal heating and external cooling two different thermal cycling configurations are possible. One configuration is to heat the specimen to a certain temperature, switch the heating off and activate the cooling until the minimal temperature is reached and the heating is switched on again. The other configuration is to keep the cooling switched on during the whole experiment (constant cooling) and switch the heater mesh frequently on and off. The maximum temperature when the heating is switched off is again controlled by embedded thermo couples. For this configuration the inhomogeneity of the temperature distribution through the specimen (thickness) is expected to be the highest. This is due to the low temperatures at the outer specimen surfaces (external cooling continuously switched on) and the higher temperatures in the inside of the specimen (internal heating switched on). However, this configuration simulates the flight conditions to the highest degree and is expected to be one of the worst case scenarios in respect to the temperature distribution.

3 EXPERIMENTAL RESULTS: TEMPERATURES DURING THERMAL CYCLING

As a trial for future thermal cycling experiments, a heated GLARE specimen was exposed to thermal cyclic loading of a maximum of 20 cycles. The temperatures were recorded using thermo couples (see Figure 3). Two sets of thermal cycling experiments were performed. In the first set external cooling and external heating and in the second set external cooling and internal heating were used for the thermal cycling experiments. The minimum temperature was defined as 0°C and the maximum temperature as 60°C. The room temperature was between 24°C and 25°C. The experiments were conducted using one layer of Peltier elements at each side of the specimen, i.e. four Peltier elements at each side of the specimen.

For the temperature control, thermo couples were used. Figure 3 depicts the position of the two thermo couples of which the temperature records are presented in this study. The thermal cycles started with the heating phase. If one of the thermo couples reached the maximum temperature of 60°C the heating was switched off and the cooling was switched on. The cooling was stopped if one of the thermo couples reached the minimum temperature of 0°C and the heating was switched on again.

3.1 Thermal cycling of GLARE

The cooling and the heating of the (heated) Glare specimen were performed using exclusively the Peltier elements, i.e. external cooling and external heating. The electrical power of the Peltier elements for cooling and heating was controlled by defining maximum values for the Amperage. The Amperage for the heating cycles was kept constant and equal to 10 A (H10A). This heating profile was combined with three different amperage for cooling power: 8 A, 10 A and 15 A. This resulted into three different amperage profiles: Heating 10 A and cooling 8 A (C8A), heating 10 A and cooling 10 A (C10A) and finally heating 10 A and cooling 15 A (C15A).

Figure 5 shows the temperatures measured by the thermo couple TC1 (Figure 5 a, b and d) and by the thermocouple applied to heat sink (Figure 5 c). The embedded thermo couple TC1 was one of the thermo couples used to control the maximum and minimum temperatures, i.e. the power supplies. Constant cycle times were reached for cooling powers of 8 A and 10 A (see Figure 5 a). The generated heat at the hot sides of the Peltier elements during the cooling cycles could be dissipated at maximum heat sink temperatures of approximately 32°C and 34°C, respectively (cf. Figure 5 c). On the contrary, for a cooling power of 15 A, the heat sink temperatures increased further with every cooling cycle. As the amount of heat which is generated at the hot side of the Peltier elements increases with the electrical power. For a cooling power of 15 A the generated heat exceeded the amount of heat which could be dissipated by the heat sinks in the current setup. Due to the increased heat sink temperatures the cooling times increased and more heat was generated (cf. Figure 5 b). Hence, the tests were stopped at the fifth thermal cycle.

Similar heating and cooling rates were achieved between the different amperage profiles H10A C8A and H10A C10A, respectively within temperatures from 25°C to 60°C (cf. Figure 5 d). The different cooling rates resulted in maximum measured temperature differences through the thickness

(out-of-plane) of up to 4°C, 6°C and 10°C for H10A C8A, H10A C10A and H10A C15A. However, the cooling rate for temperatures below 25°C was considerably lower since the temperature rate changes its behaviour from approximately linear to non-linear. This non-linear behaviour results from the increasing temperature differences at the hot and cold sides of the Peltier elements [30].

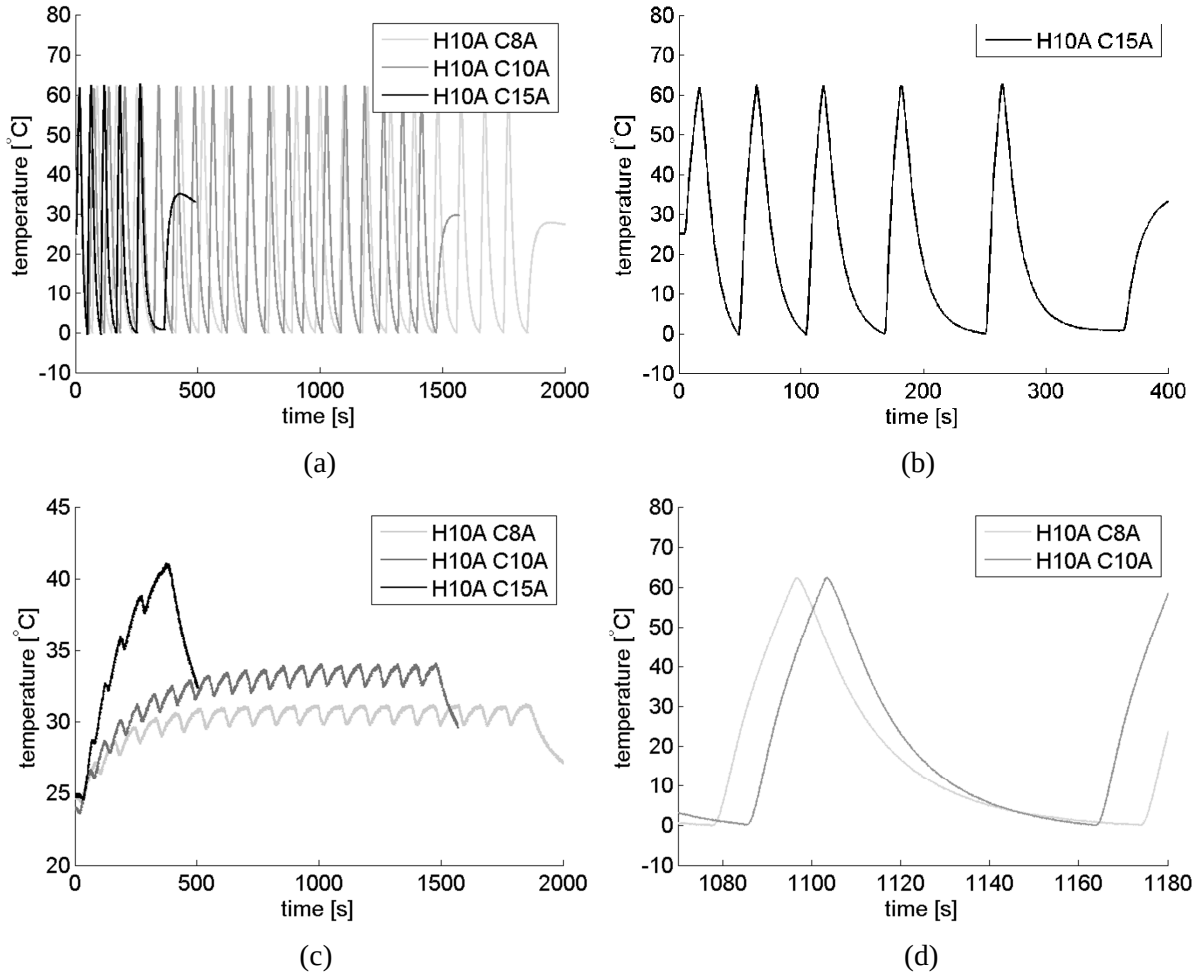

Figure 5: Temperatures during the thermal cycling (external cooling and heating) of the heated GLARE 5-4/3-0.3 specimen at (a, b, d) the embedded thermo couple TC1 and (c) the thermo coupled applied to the heat sink

3.2 Thermal cycling of heated GLARE

For this second experiment, the cooling of the specimen, which is shown in Figure 3, was performed using the Peltier elements at the external surfaces and the heating was performed using the embedded (internal) heater mesh. Thus, external cooling and internal heating were used for the thermal cycling experiments. Similarly to section 3.1, the cooling power was varied and the heating power was kept constant. The heating power was chosen with 24 A (H24A) in order to get comparable thermal cycling times as for the thermal cycling tests using external cooling and external heating.

Figures 6 a and b show the temperatures of the thermo couples TC1 and TC2, respectively during the thermal cycling tests using cooling powers (Peltier elements) of 8 A (C8A), 10 A (C10A) and 15 A (C15A). Similar to the thermal cycling tests from section 3.1 (external cooling and heating), the heat sink temperatures during thermal cycling with external cooling and internal heating did not exceed 34°C for cooling powers of 8 A and 10 A. However, the heat sink temperatures increased for a cooling power of 15 A when using external cooling and internal heating. As for higher cooling powers, the amount of heat which is generated at the hot side of the Peltier elements increases and exceeds the amount of heat which can be dissipated through the heat sinks in the current setup. Therefore, the

experiment for the configuration H24A C15A was stopped after 9 cycles.

Furthermore, Figure 6 shows that the temperature magnitudes vary through the specimen, since the temperatures measured by the two thermocouples differ significantly. As the two thermo couples TC1 and TC2 are embedded at different positions in the specimen (cf. Figure 3). It can be seen that the minimum temperatures of the configurations H24A C8A and H24A C10A were similar for both thermo couples as the cooling was performed using the Peltier elements, i.e. from outside and throughout the whole two outer surfaces. On the contrary, the maximum temperatures of the two graphs from the thermo couples at different positions differ about 25°C. The different maximum temperatures result from the internal heating using the embedded mesh. The maximum temperatures in-plane vary as a function of the distance from the embedded heater elements.

The maximum measured temperature differences through the thickness (out-of-plane) were up to 4°C, 6°C and 10°C for H24A C8A, H24A C10A and H24A C15A. Thus, the temperature distribution through and across the specimen is inhomogeneous for external cooling and internal heating. Furthermore, heating the specimens using the embedded (internal) and non-homogeneously distributed heater mesh causes edge effects, i.e. the temperatures at the specimen edges are lower than the temperatures in the specimen center.

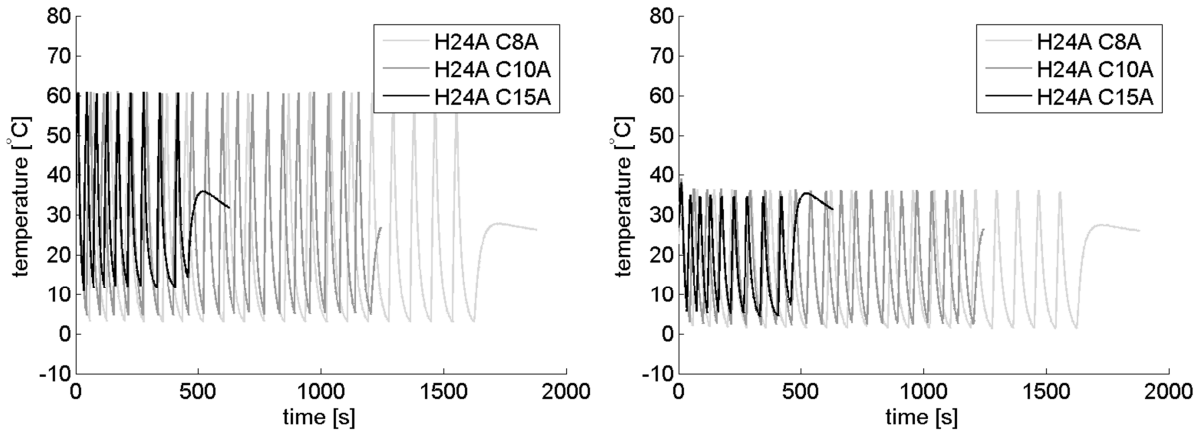

(a) (b)

Figure 6: Temperatures during the thermal cycling (external cooling and internal heating) of the heated GLARE 5-4/3-0.3 specimen at the embedded thermo couples (a) TC1 and (b) TC2

4 DISCUSSION

The specimen size is easily adoptable due to the modular experimental setup. The specimen size and the shape can be adopted by adding or removing Peltier elements. Furthermore, the variation of the number of Peltier elements enables the parallel testing of multiple specimens with the same thickness but different (thermal) load histories. This means that e.g. specimens with no significant (thermal) load history after the curing process can be thermal cycled parallel with aged samples or samples which had already been exposed to severe thermal cycling.

If future test specification for thermal fatigue tests require lower (minimal) temperatures or higher temperature change rates, two basic options are proposed. The first option is to install the experimental setup in a climate chamber with temperatures below zero. Hence, the colder ambient temperatures in cooled climate chambers allow for lower temperatures and higher cooling rates at the cold side of the Peltier elements [30]. The second option for increasing the temperature ranges and changing the temperature change rate is to stack the Peltier elements, i.e. to use two or more layers of Peltier elements. The stacking of Peltier elements decreases the effectiveness of each Peltier Element, but allows for larger temperature differences.

As no liquids are used for heating and cooling, the moisture content of the specimens is not affected by the heating and cooling devices themselves (no direct contact with e.g. a cooling liquid). However, if the moisture content of the specimen has to be kept constant or is in the focus of the examinations, the specimens can be sealed in waterproof plastic bags. Thus, water droplets due the

possible condensation of the humidity in the ambient air during the cooling phase do not affect the moisture content of the specimen.

Peltier elements have a cold and a hot side. During the cooling phase of the specimens, the cold sides of the Peltier elements are at the specimen surfaces and the hot sides are at the heat sinks. If the cooling power is chosen (too) high in respect to the heat sinks, the heat sinks heat up. The higher heat sink temperatures increase the time needed for cooling the specimens to the required minimum temperatures. If the heat sink temperatures increase during each thermal cycle further, the thermal cycling times (increase of cooling times) increase continuously. The longer cooling times cause a further temperature increase of the heat sinks and result in an unstable thermal cycling process. Thus, the amount of heat which can be transferred from the heat sinks to the air regulates the maximum cooling power. The heat transfer, i.e. the maximum cooling power, can be increase by using larger heat sinks, lower ambient air temperatures or the stacking of Peltier elements.

High temperature change rates cause a more inhomogeneous temperature distribution in the thickness direction of the specimen. Thus, for high heating and cooling powers the temperature should at least be controlled at two positions, one in the center plane and one close to the specimen surfaces. In the case of high temperature increase rates the temperature differences between the center plane and the specimen surfaces might be considerably high which leads to a non-uniform temperature distribution through the thickness. On the one hand it is likely that regions close to the heated surfaces (areas) are overheated or undercooled if the temperature is only controlled at one position in the center plane. On the other hand, if the temperature is only controlled close the heated or cooled surfaces (areas), the regions farther away from the heated or cooled regions (areas) might not reach the required temperatures. Thus, the number and position of (embedded) thermo couples which control the heating and cooling power are important design considerations.

Moreover, the (overall) exposure times to the maximum and minimum temperatures of the specimen surfaces and the layers close to the center plane differ. Thus, in case of (too) high temperature change rates the possible (aging) effects on the material characteristics are likely to be a function of the layer position in respect to the thickness. Aging effects might result from the accumulation of times where the specimens are exposed to moderate temperatures [20,22,26]. Lower temperature change rates or dwelling times with less power when the maximum or minimum temperatures are reached are proposed solutions to reach the required temperatures through the thickness without overheating or undercooling the surface areas of the specimens.

Another important issue for thermal fatigue tests is the awareness of the initial specimen conditions, i.e. the storage conditions (moisture content), defects, pre-treatments and (thermal) loading histories of the specimen, e.g. when using (heated) FMLs which were manufactured by curing in the autoclave. As the different temperature gradients of laminated materials, e.g. for the aluminium, the UD layers and the embedded mesh in heated GLARE, lead to thermal residual stresses [1]. Furthermore, the exposure of specimens to moderate temperatures might lead to aging affects, i.e. changes in the microstructure of the materials. If the specimens are pre-deformed, e.g. due to forming processes [29], mechanical residual stresses superimpose with thermal residual stresses and should be consider when evaluating the test results.

5 CONCLUSIONS

The experimental setup which was presented in this study enables different options for heating and cooling multi-functional materials (e.g. heated GLARE) using Peltier elements and embedded heater elements. One option is to provide external cooling and external heating using Peltier elements for both heating and cooling. The other option is to provide external cooling using Peltier elements and internal heating using the embedded heater meshes in e.g. heated GLARE.

The thermal cycling tests presented in this study showed that thermal cycle times of about 62 s for heated GLARE 5-4/3-0.3 and a temperature range from 0°C to 60°C specimens can be reached. The temperature distributions are more homogeneous when external cooling and external heating is provided using the Peltier elements. In the case of internal heating of the specimens using the s-shaped embedded mesh, the temperature distribution is less homogenous as the heater element acts as a local heat source and does not heat the whole surface as e.g. Peltier elements do. Thus, the temperature

needs to be measured at different positions through the thickness and at different distances from the heater mesh in order to avoid the overheating areas close to the heater mesh and to reach the required temperatures across the whole specimen.

Advantages of this experimental setup are the independent control of the heating and cooling power, i.e. temperature change rates, and the option to provide constant external cooling and at the same time provide internal heating using the embedded heater mesh. Furthermore, the experimental setup is adoptable to different specimen dimensions, enables thermal cycling of multiple specimens of the same material, allows for different temperature ranges and temperature change rates. Different temperature ranges and temperature change rates can be reached by stacking Peltier elements or by placing the experimental setup in a climate chamber with lower temperatures.

ACKNOWLEDGEMENTS

This study is partially funded by the Dutch Technology Foundation STW and Fokker Aerostructures.

REFERENCES

[1] M. Abouhamzeh, J. Sinke and R. Benedictus, Investigation of curing effects on distortion of fibre metal laminates, *Composite Structures*, **122**, 2015, pp. 546-552

[2] R. C. Alderliesten and J. J. Homan, Fatigue and damage tolerance issues of Glare in aircraft structures, *International Journal of Fatigue*, **28 (10)**, 2006, pp. 1116-1123

[3] A. G. Anisimov, B. Müller, J. Sinke and R. M. Groves, Strain characterization of embedded aerospace smart materials using shearography, Proceedings SPIE 9435, paper 943524, 2015

[4] ASTM, Standard Test Method for Short-Beam Strength of Polymer Matrix Composite Materials and Their Laminates, *ASTM standards*, D2344/D2344M-13, 2013

[5] A. A. Costa, D. F. N. R. da Silva, D. N. Travessa, and E. C. Botelho, The effect of thermal cycles on the mechanical properties of fiber metal laminates, *Materials and Design*, **42 (1)**, 2012, pp. 434-440

[6] Federal Aviation Administration (FAA), Airplane and Engine Certification Requirements in Supercooled Large Drop, Mixed Phase and Ice Crystal Icing Conditions, Federal Register 75 (124), 2010, 37311-37339

[7] Fibre Metal Laminates Centre of Competence, http://www.fmlc.nl, accessed 9.2.2015

[8] T. P. Gabb, J. Gayda and R. A. Mackay, Isothermal and Nonisothermal Fatigue Behavior of a Metal Matrix Composite, *Journal of Composite Materials*, **24**, 1990, 667-686

[9] M. S. Gale and B. W. Darvell, Thermal cycling procedures for laboratory testing of dental restorations, *Journal of Dentistry*, **27**, 1999, pp. 89-99

[10] M. Hagenbeek, *Characterisation of Fibre Metal Laminates under Thermo-mechanical Loadings*, PhD thesis, TU Delft, 2005

[11] P. Hofslagare, Residual Stress Measurement on Fibre metal-laminates, *Journal of Neutron Research*, **11 (4)**, 2003, pp. 215-220

[12] L. A. Knobloch, D. Gailey, S. Azer, W. M. Johnston, N. Clelland and R. E. Kerby, Bond strengths of one- and two-step self-etch adhesive systems, *The Journal of Prosthetic Dentistry*, **97 (4)**, 2007, pp. 216-222

[13] LabView http://www.ni.com/13/, accessed 9.2.2015

[14] H. Mang and G. Hofstetter, *Festigkeitslehre*, Springer Wien New York, 2008

[15] M. Liu, W. Saman and F. Bruno, Review on storage materials and thermal performance enhancement techniques for high temperature phase change thermal storage systems, *Renewable and Sustainable Energy Reviews*, **16**, 2012, pp. 2118-2132

[16] M. Mohseni, and A. Amirfazli, A novel electro-thermal anti-icing system for fiber-reinforced polymer composite airfoils, *Cold Regions Science and Technology*, **87**, 2013, pp. 47-58

[17] B. Müller, S. Teixeira De Freitas and J. Sinke, Measuring thermal diffusion in fiber metal laminates, Proceedings of the ICAST2014: 25th International Conference on Adaptive Structures and Technologies, paper 76, 2014

[18] T. Nikaido, K.-H. Kunzelmann, H. Chen, M. Ogata, N. Harada, S. Yamaguchi, C. F. Cox, R. Hickel and J. Tagami, *Evaluation of thermal cycling and mechanical loading on bond strength of a self-etching primer system to dentin, Dental Materials*, **18**, 2002, pp. 269-275

[19] J. H. L. Pang, D. Y. R. Chong and T. H. Low, Thermal Cycling Analysis of Flip-Chip Solder Joint Reliability, *IEEE transactions on components and packaging technologies*, **24 (4),** 2001, pp. 705-712

[20] G.M. Odegard and A. Bandyopadhyay, Physical Aging of Epoxy Polymers and Their Composites, *Journal of Polymer Science Part B: Polymer Physics*, **49 (24)**, 2011, pp. 1695-1716

[21] Y. Qi, R. Lam, H. R. Ghorbani, P. Snugovsky and J. K. Spelt, Temperature profile effects in accelerated thermal cycling of SnPb and Pb-free solder joints, *Microelectronics Reliability*, **46**, 2006, pp. 574-588

[22] S. Rajasekaran, N. K. Udayashankar and J. Nayak, T4 and T6 Treatment of 6061 Al-15 Vol.% SiCp Composite, *ISRN Material Science*, ID 374719, 2012, pp. 1-5

[23] G. H. J. J. Roebroeks, *Towards GLARE the development of a fatigue insensitive and damage tolerant aircraft material*, PhD thesis, TU Delft, 1991

[24] H.-C. Shih, N.-J. Ho and J. C. Huang, Precipitation Behaviours in Al-Cu-Mg and 2024 Aluminum Alloys, *Metallurgical and materials transactions A*, **27**, 1996, pp. 2479-2494

[25] T. Shimokawa, H. Katoh, Y. Hamaguchi, S. Sanbongi, H. Mizuno, H. Nakamura, R. Asagumo, H. Tamura, Effect of Thermal Cycling on Microcracking and Strength Degradation of High-Temperature Polymer Composite Materials for Use in Next-Generation SST Structures, J*ournal of Composite Materials*, **36 (7)**, 2002, pp. 885-895

[26] G. W. Stickley and H. L. Anerson, Effects of Intermittent Versus Continuous Heating upon the Tensile Properties of 2024-T4, 6061-T6 and 7075-T6 Alloys, *NACA technical memorandum 1419*, 1956

[27] C. Vermeeren, *Around Glare – a new aircraft material in context*, Kluwer Academic Publishers, Dordrecht, 2002

[28] A. Vlot, *Glare – history of the development of a new aircraft material*, Kluwer Academic Publishers, Dordrecht, 2001

[29] A. Vlot and J. W. Gunnink. *Fibre metal laminates – an introduction*, Kluwer Academic Publishers, Dordrecht, 2001

[30] D. D. L. Wijngaards, E. Cretu, S. H. Kong and R. F. Wolffenbuttel, Modelling of integrated Peltier elements, Proceedings of the 3rd International Technical Conference on Modelling and Simulation of Microsystems, 2000, pp. 652-655